Examining the Impact of Microphysics Parameterizations in Simulations of a Vermont Winter Storm

Michael L. Wasserstein

Department of Physics, Middlebury College, Middlebury, VT

Project report for PHYS 0704

July 7, 2021

Abstract

Using the Weather Research and Forecasting (WRF) Model, we conducted simulations of a major winter storm that produced up to 50 centimeters of snow in parts of Vermont (VT) on 20-21 January 2019. In WRF simulations, different microphysics parameterizations (MP) yield different model outputs of sizes and fall velocities of atmospheric particles. We employed a sensitivity test using the Morrison 2-moment (M2M), Thompson (THOM), WRF Double Moment 6-class (WDM6), Milbrandt–Yau (MILL), and Goddard (GODD) MPs to analyze snowfall during the Vermont storm, and we compared our results to real observations at a near sea level site in Middlebury, VT, and a mountain location in Rochester, VT. We analyzed snowfall mixing ratios and accumulated snowfall totals predicted by WRF to find that the THOM and GODD MPs predicted snowfall totals that fell most in line with observed snowfall from the storm, while M2M slightly overpredicted snowfall, WDM6 slightly underpredicted accumulated snow, and the MILL simulation grossly underpredicted snowfall but predicted a large accumulation of graupel, causing total accumulated precipitation to be fairly accurate.

Date Accepted: _____

Table of Conetnts

I Introduction

Vermont (VT), located in the northeast of the United States, is a state susceptible to major winter storms, as a result of its northerly latitude, the Green Mountain Range that bisects its center from north to south, and Lake Champlain, which lies on the state's eastern border with New York. These storms have important implications for the state, bolstering its economy through winter recreation, while causing damage to infrastructure and affecting people's lives. In the present study, we considered one of these storms that impacted the state in January 2019 by analyzing the physics of the clouds throughout the duration of the storm.

I. (i) The Storm

During the period from 20 January to 21 January 2019, a major winter storm produced up to 50 centimeters of snow in parts of Vermont [1]. At Burlington International Airport (BTV) in South Burlington, VT, where the state's primary first order weather station is located, 47.2 cm of snow fell from this storm, making it the 18th largest snowstorm on record at BTV and the 5th largest in January. At the storm's peak intensity during the morning on 20 January, the snowfall rate reached 6.1 cm per hour. Temperatures were unusually cold for a snowstorm of this magnitude, falling below -20 °C for much of the day on 20 January and through the morning on 21 January. Despite the arctic air that was in place, snow-to-liquid ratios were relatively low at roughly 10:1 for the majority of the storm, though they did increase as it progressed. Impacts of the storm were primarily travel related, as it coincided Martin Luther King Jr. Day weekend, a popular weekend for New England skiers to travel to Vermont. With nearly 50 cm of snow falling in a 24 hour period in spite of low snow-to-liquid ratios, the microphysical conditions of the clouds were ripe for producing snow and contributed to the heavy snowfall rates that occurred. Past research on cloud microphysics of Vermont winter storms is scarce, and forecast skill for these storms varies frequently, providing motivation for this study.

I. (ii) Cloud Microphysics

Clouds contain water droplets and ice particles that are suspended in air, and cloud microphysics is the study of the microscale processes occurring within these small particles that make up clouds [2]. The dynamics of cloud microphysics begins with a cloud condensation nucleus (CCN), a particle with a diameter on the order of 1 μm, that provides an ideal surface for other water droplets to stick to. As more water particles coalesce to the original CCN, a cloud particle forms, and more particles combine until a rain drop or snowflake is formed, as shown in Fig. 1. For rain drops to fall, the saturation ratio,

$$S = \frac{e}{e_S}, \tag{1}$$

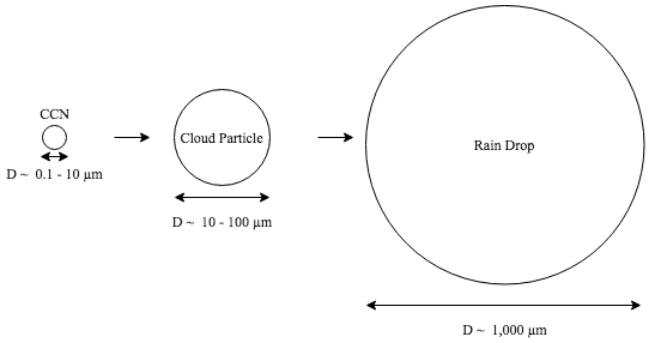

Fig. 1. The dynamics of cloud microphysics. A cloud condensation nucleus (CCN), a tiny water particle with diameter $D \sim 0.1$ - 10 μm, provides a surface to which other water particles can stick. These other particles combine with the original CCN and cause it to grow, forming a cloud particle and ultimately a rain drop with $D \sim 1{,}000$ μm. When the atmosphere becomes saturated, these rain drops fall, causing precipitation.

where e is the water vapor pressure and e_S is the saturation vapor pressure, must equal 1. When $S = 1$, the atmosphere becomes saturated and it cannot hold any additional moisture, causing particles to fall as precipitation. Cloud microphysics has important implications on the weather that we experience every day.

In numerical weather prediction (NWP), cloud microphysics is one of the many variables that we must take into account when predicting precipitation, and there are numerous ways to parameterize cloud microphysics. Microphysical modeling consists of different schemes that have either a bin or bulk structure. Bin schemes, while computationally more expensive and complex, can be much more effective because they divide cloud particles into thousands of bins and model what a particle does based on each individual bin [3]. On the flip side, bulk microphysics schemes, which are used more widely in operational weather models, use an empirical gamma or exponential distribution to determine particle sizes based on a prognosticated total number concentration N_T and/or mixing ratio q in the atmosphere [3, 4]. Here N_T is a measure of the number of particles of diameter D of a given hydrometeor compared to all particles in the atmosphere, while q is the ratio of the mass of particles of a given hydrometeor to the mass of the atmosphere.[1] While a bin scheme individually determines particle sizes for each bin, a bulk scheme uses a distribution to make this determination. A gamma particle size distribution in a bulk scheme can take the form

$$N(D) = N_0 D^{\alpha} e^{-\lambda D}, \tag{2}$$

where $N(D)$ is the total number concentration per unit volume of particles of diameter D, and N_0,

[1] A hydrometeor is a type of particle in the atmosphere, such as hail, water vapor, rain, or snow.

λ, and α are the intercept, slope, and shape parameters of the size distribution, respectively [5]. The parameters N_0 and λ can be determined by predicted values for N_T and q in the bulk scheme, while α depends on the hydrometeor examined. As an example of how the parameters in Eq. 2 could be determined, the intercept parameter can be given by

$$N_0 = N_T \frac{1}{\Gamma(1+\alpha)} \lambda^{1+\alpha}, \tag{3}$$

and the slope parameter could be given by

$$\lambda = [\frac{\Gamma(1+d+\alpha)}{\Gamma(1+\alpha)} \frac{cN_T}{\rho q}]^{1/d}, \tag{4}$$

where d and c are constants that depend on the hydrometeor and ρ is the density of air. Equations 3 and 4 are calculated for each hydrometeor category, and in most MPs, α is a fixed value, while q and N_T can vary. By making a prediction about q and N_T and holding α constant, a microphysics scheme could use equations like Eqs. 3 and 4 to determine N_0 and λ, respectively, in order to determine the particle size distribution given in Eq. 2.[2]

Each microphysics scheme has a moment, which is the number of prognostications it makes in its particle size distribution. For example, a single-moment scheme might only predict q (leaving N_T and α fixed), while a double-moment scheme could predict N_T and q, which are input into equations that determine N_0 and λ in Eq. 2. A rare three-moment scheme predicts N_T, q, and α, rather than leaving the shape parameter α fixed. Based on the determined particle size distribution in Eq. 2, the bulk scheme will predict the particle size, underpinning cloud microphysics modeling in NWP.

The Advanced Research Weather Research and Forecasting Model (WRF) is a community atmospheric modeling system that allows users to model many physical, dynamical, and chemical processes in the atmosphere through real or idealized simulations [6]. In WRF, users can choose between many microphysics parameterizations (MPs) that use either empirical gamma or exponential distributions to determine particle size for different hydrometeors based on assumptions about mixing ratios or number concentrations (see Eq. 2). In previous WRF simulations of real winter storms, common MP choices include the Morrison 2-moment (M2M), Thompson (THOM), WRF Double Moment 6-class (WDM6), Milbrandt–Yau Double Moment (MILL), and Goddard (GODD) microphysics schemes [4, 5, 7–11]. Table I summarizes the characteristics of these 5 MPs. Because they make different predictions about q and N_T for each hydrometeor, when chosen as an MP in WRF, each of these bulk schemes should yield different outputs when the model is run. In this paper, we seek to examine the model outputs for these 5 microphysics schemes, using the January 2019 Vermont winter storm as our case study.

[2]Note that we intentionally use vague language here, since each MP has its own equations and not all follow Eqs. 3 and 4 exactly when determining parameters for its particle size distribution.

Table I. An overview of the Morrison 2-moment (M2M), Thompson (THOM), WRF Double Moment 6-class (WDM6), Milbrandt–Yau Double Moment (MILL), and Goddard (GODD) microphysics schemes in the Weather Research and Forecasting Model. For each scheme, the moment, prognostic mass variables q, and prognostic number variables N_T are listed. The subscripts c,r,i,s,g,h, and n correspond with cloud, rain, ice, snow, graupel, hail, and cloud condensation nuclei, respectively. The units $\mathrm{kg\ kg^{-1}}$ and $\mathrm{kg^{-1}}$ are units of the default outputs in the WRF model.

	Moment	Mass variables q ($\mathrm{kg\ kg^{-1}}$)	Number variables N_T ($\mathrm{kg^{-1}}$)
M2M	2	q_c, q_r, q_i, q_s, q_g	N_r, N_i, N_s, N_g
THOM	hybrid	q_c, q_r, q_i, q_s, q_g	N_i, N_r
WDM6	2	q_c, q_r, q_i, q_s, q_g	N_n, N_c, N_r
MILL	3	q_c, q_r, q_i, q_s, q_g, q_h	N_c, N_r, N_i, N_s, N_g, N_h
GODD	1	q_c, q_r, q_i, q_g, q_s, q_h	

II Methods

To analyze the cloud microphysics of the January 2019 Vermont winter storm we used the Advanced Research Weather Research and Forecasting Model version 4.2.1. The model was configured with 10 km horizontal grid spacings for 38 levels in the atmosphere above mean sea level (MSL). Each simulation was initialized using Global Forecast System (GFS) analysis data with a 0.5° grid increment obtained from the National Centers for Environmental Information (NCEI) GFS database [12]. The GFS analysis data set the initialized conditions for the land surface, atmosphere, and boundary at 3 hour intervals.

We configured WRF using the RRTMG longwave and shortwave parameterizations, the Noah-MP Land Surface Model, and Yonsei University planetary boundary layer parameterization, which remained constant for all of our experiments. For an overview of each of these parameterizations, see the WRF users guide [6]. We varied MPs, using M2M, THOM, WDM6, MILL, and GODD, which are described in greater detail in Table I. For each simulation, we ran WRF for 48 hours from 0000 UTC 20 January 2019 to 0000 UTC 22 January 2019. Although there were minimal snow accumulations on 21 January 2019, we focused data analysis entirely on 20 January 2019, when the brunt of the snow in this storm fell. We analyzed the region shown in Fig. 2, which contains 17 longitudinal segments and 24 latitudinal segments, for a total of 408 gridpoints on the 2-dimensional plane. Each gridpoint also contains data for 38 levels of the atmosphere extending to 20,000 meters above the surface of the earth. We obtained NetCDF output files for each hour during which simulations were run. To compare each simulation, we considered estimated radar reflectively data, mixing ratio data for all hydrometeors at

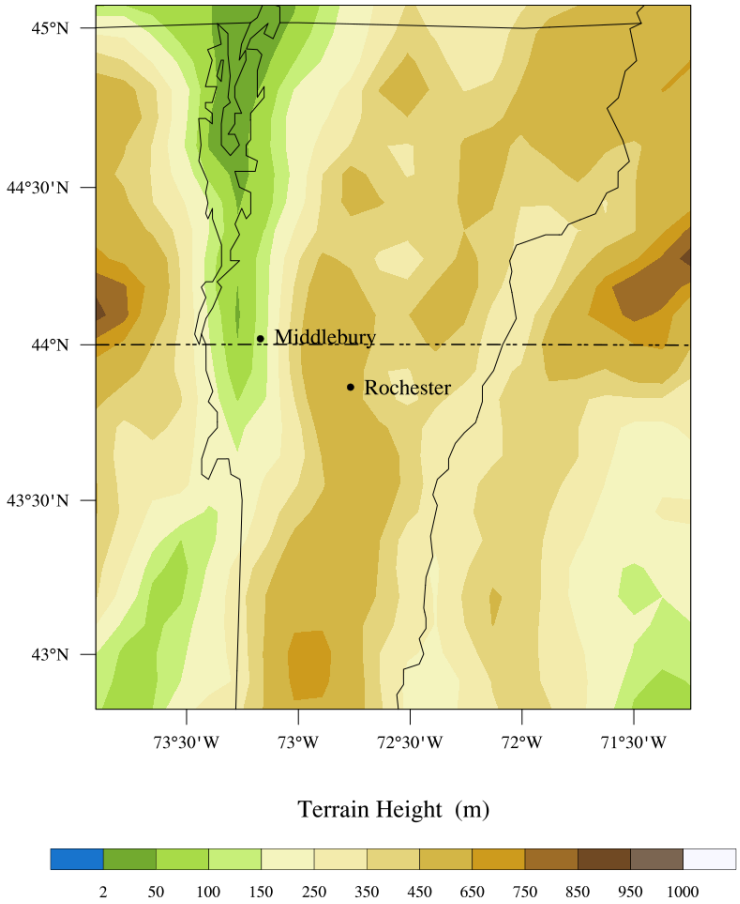

Fig. 2. Terrain height for the domain for data analysis. For our study, we took averages of all gridpoints contained in this domain. The domain contains 17 longitudinal segments and 24 laditudinal segments, giving a total of 408 gridpoints on the 2-dimensional plane. We also examined data at Middlebury and Rochester, the two labeled towns, and compared these results to real observations from the storm. The dashed horizontal line is the line across which we analyzed snow mixing ratio vertical cross sections.

different levels of the atmosphere, and accumulated snowfall. Following National Weather Service (NWS) observations reporting that snow-to-liquid ratios remained near 10:1 for the storm's duration, we assumed a 10:1 ratio for our analysis [1]. We used the mixing ratio data to draw assumptions about accumulated snowfall and compared snowfall data to real storm observations from Community Collaborative Rain, Hail & Snow (CoCoRaHS) Network sites in Middlebury, VT (MSL 113 m) and Rochester, VT (MSL 527 m).

III Results

III. (i) Accumulated Snowfall

Observed snowfall totals for the Vermont January 2019 snowstorm ranged from 25 to 50 cm, and as shown in Fig. 3, total accumulated snowfall S_a for our simulations falls roughly in line with actual snowfall totals. Because of the cold, arctic air that was in place for this storm, there was not much

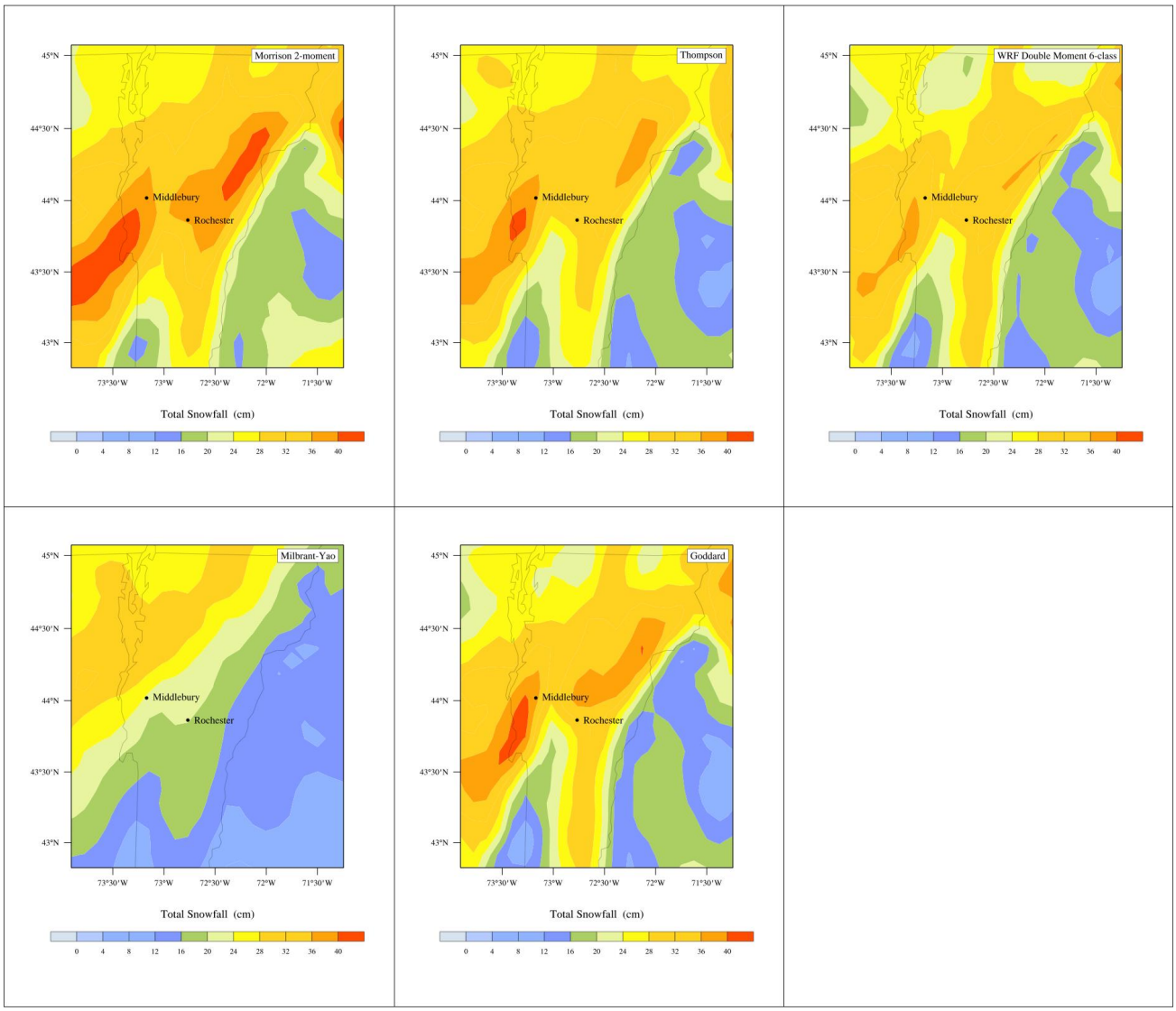

Fig. 3. Total snowfall for each MP on 20 Jan 2019. Most snowfall accumulations fall in line with storm observations, and the Milbrandt-Yao MP grossly underpredicts snowfall.

mountain enhancement of snowfall totals, which tends to happen during warmer Vermont snowstorms when mountain temperatures are much colder than temperatures in the valleys. The warm waters in the Connecticut River on the eastern VT border do appear to have some influence on snowfall totals there, as all snowfall maps in Fig. 3 show much less accumulation near and east of the river than in the

Green Mountains of central VT. A quick glance at these maps reveals that MILL predicted the least amount of snow, while M2M forecasted the most, followed by THOM, WDM6, and GODD, which each predicted roughly the same amount of snowfall. The darker segments of red in M2M, THOM, and GODD simulations show where some heavier bands of snow may have set up during the morning hours on 20 January 2019.

Figure 4 shows the development of the snowstorm for each simulation during the first 24 hours using an average accumulated snowfall $\overline{S_a}$ for all gridpoints in our domain. As the accumulation maps in Fig. 3 also confirm, MILL predicted the least amount of snow for the entire domain, while M2M predicted the most. Snowfall gradually began to accumulate at 0000 UTC on 20 January 2019 before

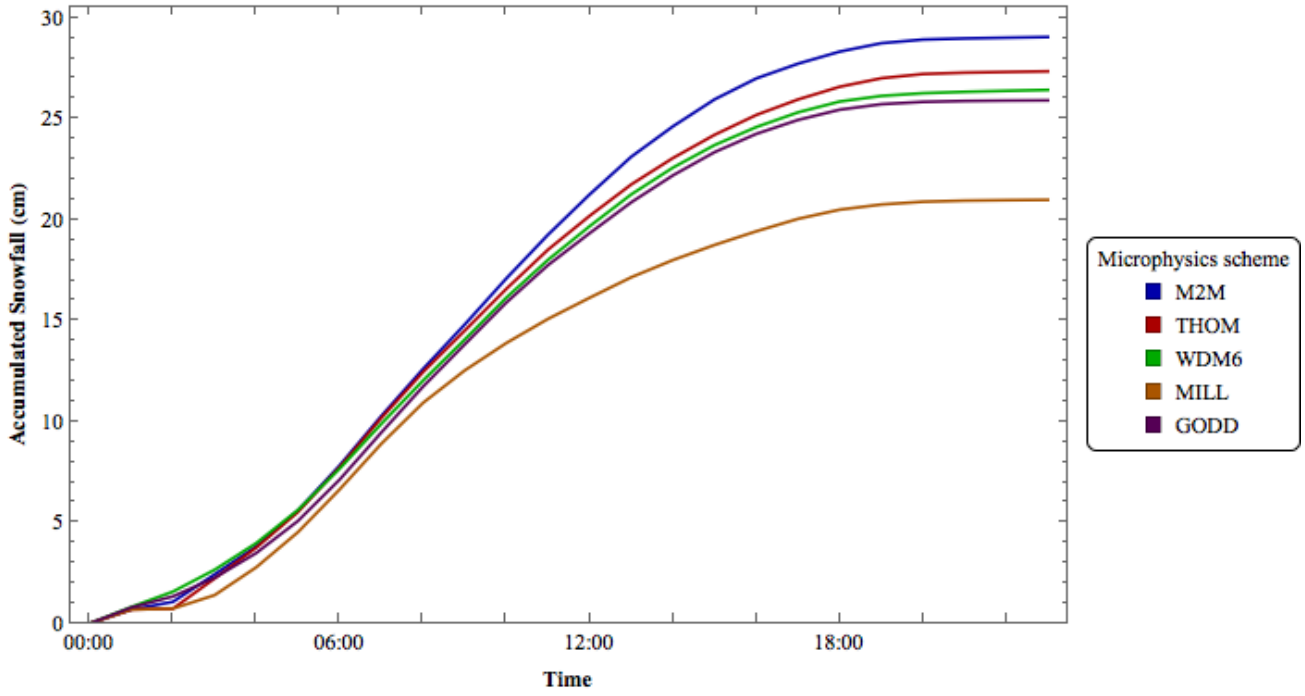

Fig. 4. Total accumulated snowfall during 20 Jan 2019. The data points in this figure were obtained by averaging accumulated snowfall for all grid points in our domain for data analysis. The fastest accumulations occurred during the morning on 20 Jan 2019, before snow tapered off during the late afternoon.

increasing to its greatest rates in the overnight hours and continuing throughout the day before tapering off during the late afternoon. While the MILL simulation has fairly similar S_a to other MPs during the early parts of the storm, accumulation begins to slow earlier than all other MPs, which could explain why MILL predicted the least snow. On the contrary, M2M predicted snow to continue at a steady rate before tapering off at around 1400 UTC, resulting in a larger total accumulation than any other simulation.

Table II shows total snow accumulations S_a for Middlebury (MSL 113 m) and Rochester (MSL

527 m), VT, as well as the mean of all gridpoints for our domain (Fig. 2). In Middlebury, all simulations underpredicted S_a compared to the actual observation of the storm, though the actual observation falls within the range of uncertainty for M2M, THOM, and GODD. Following general trends in the simulations, MILL grossly underpredicted snowfall in Middlebury. Compared to Middlebury, S_a as predicted by the MPs is $\sim$ 5 cm less in Rochester. While M2M only predicted 2.13 fewer cm of snow in Rochester than in Middlebury, GODD and THOM predicted 5.53 cm and 6.22 cm less, respectively, highlighting possible mountain biases in M2M. Forecast skill for THOM, WDM6, and MILL was very high at Rochester, as these simulations predicted S_a within 0.46 cm of the actual observation of S_a = 30.5 cm. Following the trends for the specific locations of Middlebury and Rochester, the average of

Table II. Total accumulated snowfall for the snowstorm on 20 January 2021 for each MP, and actual storm observations from CoCoRaHS sites. Data for Middlebury and Rochester contain the average of the nearest 5 gridpoints to the CoCoRaHS sites, and data for the domain contain the average of all grid points in the domain (Fig. 2).

	Acumulated Snowfall (cm)		
	Middlebury	Rochester	Domain
M2M	38.02 $\pm$ 1.854	35.89 $\pm$ 1.867	29.04 $\pm$ 5.000
THOM	36.26 $\pm$ 3.111	30.04 $\pm$ 2.225	27.35 $\pm$ 4.450
WDM6	34.13 $\pm$ 2.837	30.75$\pm$ 2.793	26.43 $\pm$ 4.592
MILL	23.79 $\pm$ 2.425	19.68 $\pm$ 1.015	20.98 $\pm$ 6.374
GODD	36.15 $\pm$ 4.652	30.62 $\pm$ 3.592	25.91 $\pm$ 4.626
Observation	38.1	30.5	

all gridpoints in our domain show that M2M predicted the largest $\overline{S_a}$, while MILL predicted the least snowfall. With a standard deviation of σ = 6.374 cm, MILL had the largest variability in $\overline{S_a}$, which is apparent in Fig. 3, since predicted snowfall for MILL varies largely from the northwest part of the domain to the southeast.

III. (ii) Snow Mixing Ratios

Each MP prognosticates snow mixing ratios q_s for different levels of the atmosphere. Figure 5 shows vertical profiles of snow mixing ratios at 0500, 1100, 1700, and 2300 UTC. Consistent with the accumulation of snowfall over time shown in Fig. 4, q_s peaked for all MPs at roughly 0600 UTC 20 January 2019 and gradually fell as the day and storm progressed. At 0500 UTC, all MPs had snow mixing ratios peak in the lower atmosphere at heights between 2,500 and 4,000 m above Earth's surface. MILL had the greatest q_s at this time at any level of the atmosphere, but its snow mixing ratio decreased in the lower parts of the atmosphere more rapidly than any other MP. This finding is especially evident

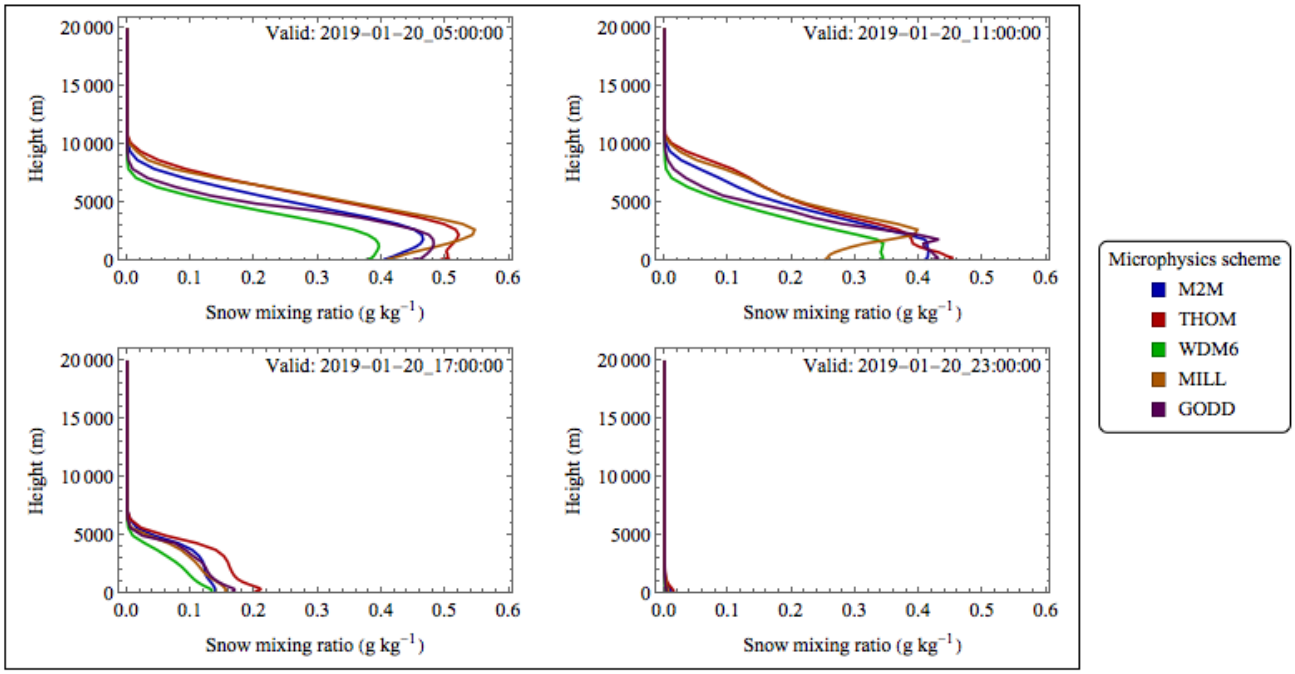

Fig. 5. Vertical profiles of snow mixing ratios for the data analysis domain at 0500, 1100, 1700, and 2300. For all MPs, snow mixing ratios q_s peaked in the morning hours on 20 Jan 2019 before tapering off by the afternoon.

at 1100 UTC in Fig. 5, where the brown line corresponding with MILL shows q_s decreasing rapidly at levels of the atmosphere below 3,000 m, while other MPs have q_s remain roughly constant or even increase in the lower atmosphere. At all times and heights in the atmosphere throughout the storm, WDM6 prognosticated the lowest q_s, except at instances in the lower levels of the atmosphere when MILL predicted a smaller q_s than WDM6.

Figure 6 shows snow mixing ratios q_s at 0500 UTC 20 January 2019 along the latitude 44 °N (see dashed line in Fig. 2) for all longitudes in our domain for data analysis. At 0500 UTC, when the snowstorm neared its peak intensity, all MPs prognosticated a large mass of snow particles in the eastern part of our domain at levels of the atmosphere < 5,000 m above Earth's surface. Mean snow mixing ratios predicted by WDM6 and GODD for this cross section at all levels of the atmosphere were $\overline{q_s}$ = 0.0142 g kg^{-1} and $\overline{q_s}$ = 0.0254 g kg^{-1}, respectively, whereas $\overline{q_s}$ was much larger for M2M, THOM, and MILL, at $\overline{q_s}$ = 0.0449 g kg^{-1}, $\overline{q_s}$ = 0.0531 g kg^{-1}, and $\overline{q_s}$ = 0.0655 g kg^{-1}, respectively. Snow mixing ratios for WDM6 and GODD are noticeably less in the center of the cross section, where Vermont's mountains are located.

Figure 7 shows the same data as Fig. 6, except 6 hours later at 1100 UTC. At this time, bands

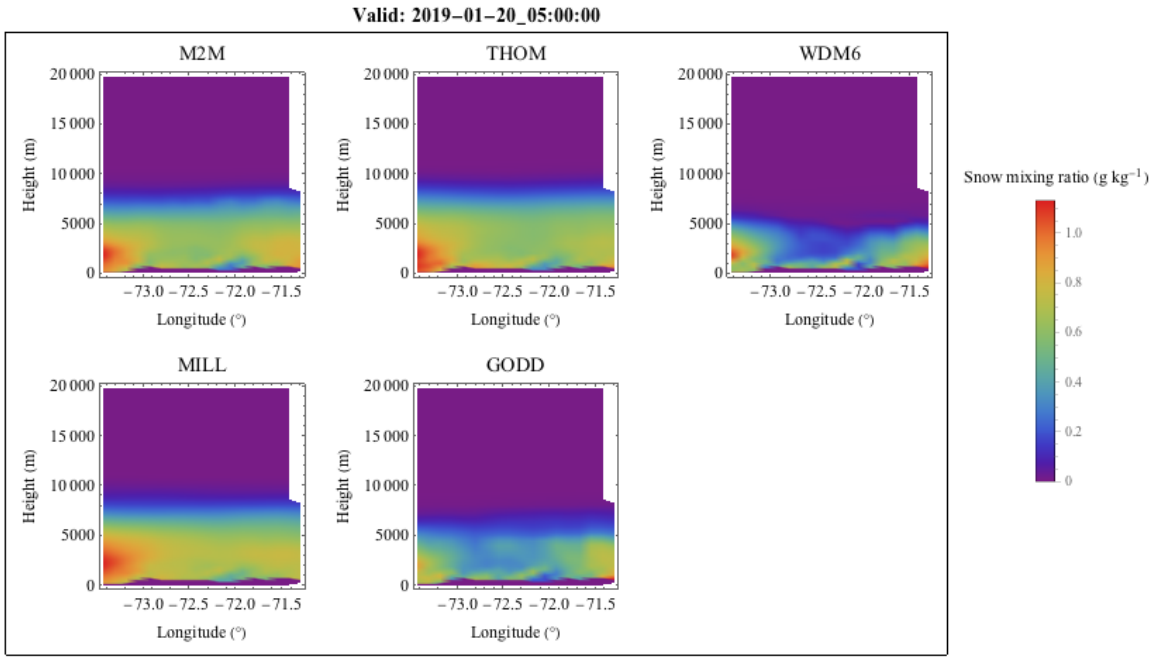

Fig. 6. Vertical cross sections at latitude 44 °N for snow mixing ratio q_s at 0500 UTC on 21 Jan 2019.

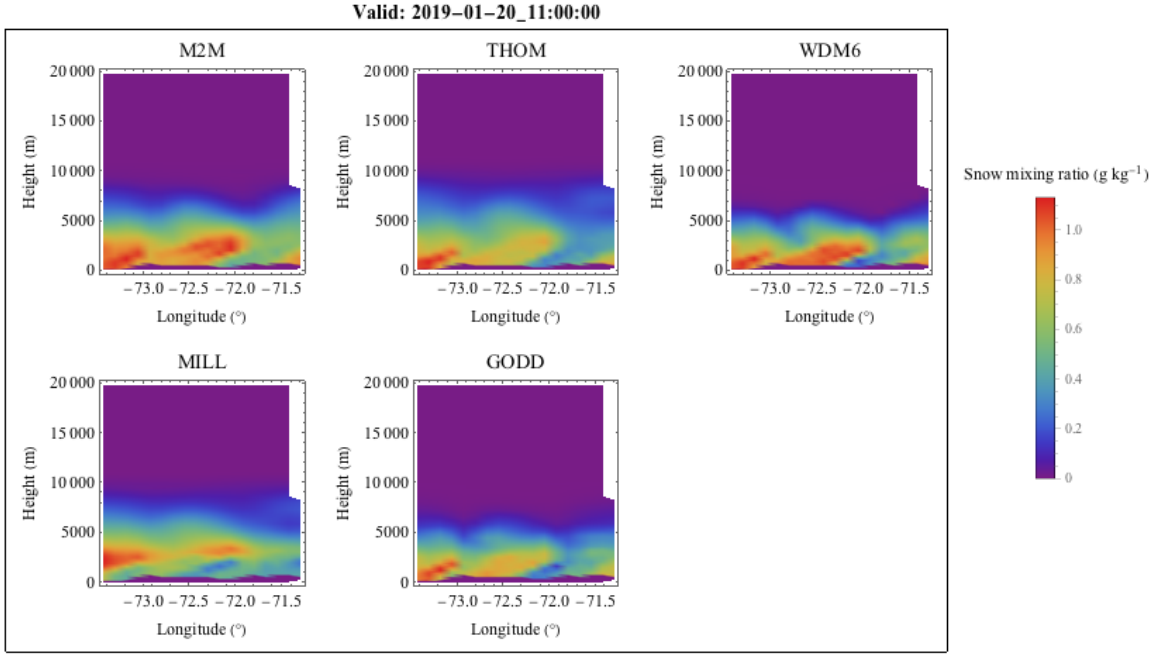

Fig. 7. As in Fig. 6, but at 1100 UTC.

of snow developed in the eastern part of the domain and in the center. The eastern band is especially apparent for all simulations, while the band that developed in the center of the state was better predicted by M2M, MILL, and WDM6 for this cross section. The cross section shown in Fig. 7 demonstrates the usual drop-off of q_s in the lower atmosphere for MILL, as peak snow mixing ratios occur at a height near 3500 m. No other MPs show this same trend; high snow mixing ratios can be found close to the surface of the earth for all other simulations. The mean snow mixing ratios $\overline{q_s}$ were higher at 1100 UTC for all simulations than at 0500 UTC, partially due to the bands of snow that formed, and partially do to the increased concentration of snow particles in the lower atmosphere. Mean values were $\overline{q_s}$ = 0.1087 g kg^{-1}, $\overline{q_s}$ = 0.1236 g kg^{-1}, $\overline{q_s}$ = 0.0749 g kg^{-1}, $\overline{q_s}$ = 0.1123 g kg^{-1}, and $\overline{q_s}$ = 0.1095 g kg^{-1} for M2M, THOM, WDM6, MILL, and GODD, respectively. WDM6 and GODD both predicted few particles in the upper atmosphere above 6,000 m at both 0500 UTC and 1100 UTC, as evidenced by the purple shade above 6,000 m in Figs. 6 and 7.

Overall, the MPs show fairly similar tendencies for snow mixing ratios, with the outlier being MILL and its rapid snow mixing ratio dropoff in the lower atmosphere. WDM6 consistently predicted the least mass of snow particles in the atmosphere, while MILL tended to predict the greatest snow mixing ratios for the upper atmosphere, and GODD and THOM predicted the the largest mass of snow particles in the lower atmosphere. The prognostication of snow mixing ratios by each MP has important implications on snowfall accumulations and rates, impacting forecast skill in meteorology.

III. (iii) Graupel

The Milbrandt-Yao microphysics scheme predicted much less snowfall and lower snow mixing ratios in the lower atmosphere than all other MPs. Out of all MPs examined in this study, MILL contains the most mass variables to predict q and more number variables to predict N_T than any other MP (See Table I). We considered why MILL predicted a significantly lower accumulated snowfall S_a than all other MPs, and its overprediction of graupel, a hydrometeor distinct from snow that can still stick to the ground, appears to be the answer. Graupel forms when supercooled water droplets freeze to snowflakes, falling to the earth as particles similar to hail or ice pellets, but with lower density. Figure 8 shows graupel mixing ratios q_g at 1100 UTC, and MILL prognosticated significantly more graupel particles than any other MP at this time and all other times. When comparing Fig. 8 to the 1100 UTC plot in Fig. 5 we can conclude that MILL's low prediction of snow particles is compensated for by its high prediction of graupel particles in the lower atmosphere. The relatively high graupel mixing ratios q_g and low snow mixing ratios q_s as predicted by MILL are especially apparent in Fig. 9, which shows that the mass of snow particles in the lower atmosphere decreases as height decreases, while the mass of graupel particles increases as height decreases. This phenomenon occurs at both 1100 UTC, when the storm was near its greatest strength, and it also occurs as the storm began to taper off at 1400 UTC.

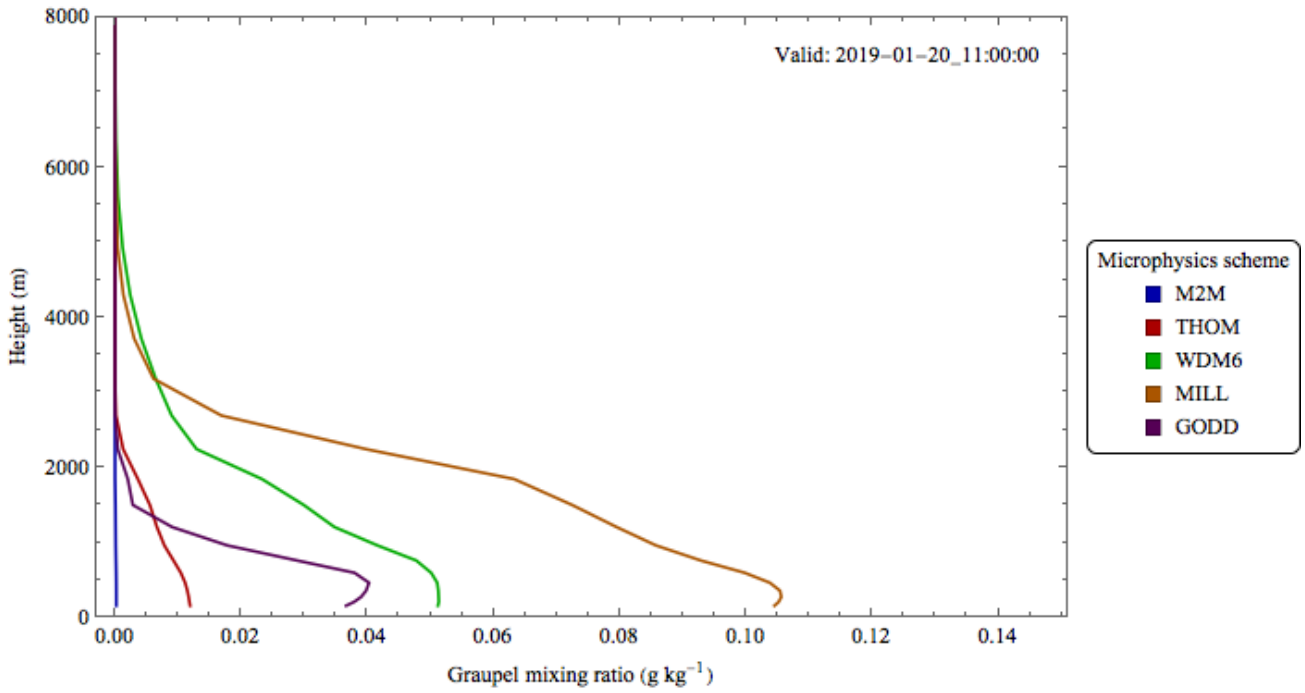

Fig. 8. Vertical profile of graupel mixing ratio q_g for the domain at points lower than 8,000 m at 1100 UTC 20 Jan 2019. MILL predicts the largest number of graupel particles in the lower atmosphere at this time, a limiting factor in its prediction of snow particles in the lower atmosphere (see Fig. 5).

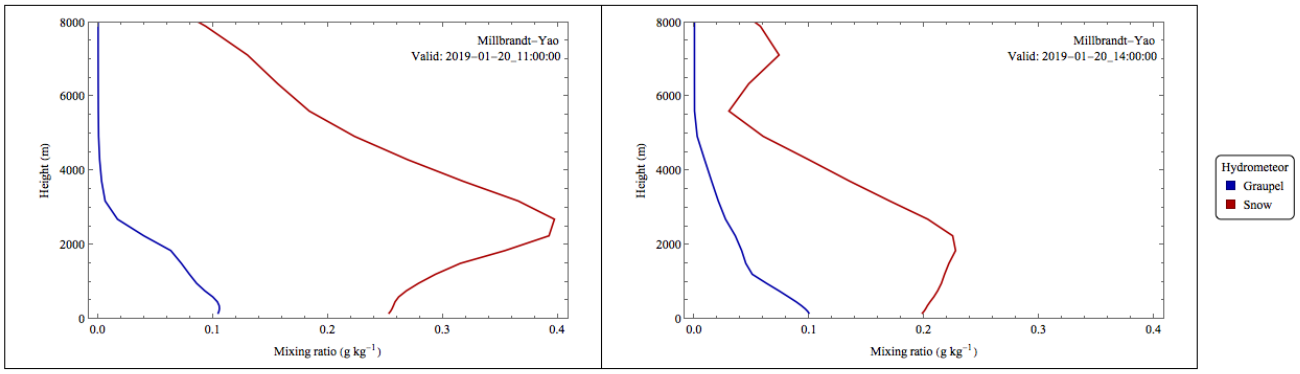

Fig. 9. Vertical profiles of graupel mixing ratio q_g and snow mixing ratio q_s for the domain at points lower than 8,000 m at 1100 UTC Jan 20 2019 and 1400 UTC Jan 20 2019 for the Milbrandt-Yao MP. Contrasting trends seen in other MPs, q_s decreases in the lowest part of the atmosphere in the MILL simulation, and q_g increases as height decreases.

Total accumulated precipitation data also show that MILL underpredicted snowfall in the storm due to its large prediction of graupel in the lower atmosphere. When we consider total accumulated precipitation P_a by summing snowfall accumulation and graupel accumualtion as predicted by WRF, MILL predicted P_a that is similar to all other MPs and the actual observations for the storm, as shown in Table III. Accumulated precipitation due to snow and graupel in Middlebury for MILL was P_a =

37.24 $\pm$ 1.580 cm, so the actual observation of P_a = 38.1 cm falls within the range of uncertainty. And in Rochester, MILL actually overpredicted total accumulated precipitation. When we consider only snowfall in Rochester, S_a = 19.68 $\pm$ 1.015 cm, but with both snow and graupel, MILL predicted an additional 13.51 cm of precipitation, causing total accumulated precipitation to be P_a = 33.19 $\pm$ 2.337 cm, when the actual observation at Rochester was P_a = 30.5 cm. Averaged over our domain for

Table III. As in II, but we included accumulated grapuel as well to calculate accumulated precipitation P_a. The column %Graupel indicates the percentage of P_a for the domain that falls as graupel. When we include graupel, MILL predicts accumulated precipitation much closer to the actual observations in Middlebury and Rochester, but a very large percentage of that precipitation falls as graupel.

	Acumulated Precipitation (cm)			
	Middlebury	Rochester	Domain	% Graupel
M2M	38.02 $\pm$ 1.854	37.21 $\pm$ 1.857	29.16 $\pm$ 5.966	0.383%
THOM	36.40 $\pm$ 3.047	34.85 $\pm$ 2.789	28.55 $\pm$ 4.008	4.22%
WDM6	36.99 $\pm$ 3.150	37.74 $\pm$ 3.141	28.96 $\pm$ 5.224	8.76%
MILL	37.24 $\pm$ 1.580	33.19 $\pm$ 2.337	28.23 $\pm$ 4.671	25.7%
GODD	36.45 $\pm$ 4.467	34.68 $\pm$ 3.532	27.13 $\pm$ 4.246	4.51%
Observation	38.1	30.5		

data analysis, MILL predicted a mean accumulated snowfall of $\overline{S_a}$ = 20.98 $\pm$ 6.374 cm. But MILL predicted that over 7 cm of graupel fell during the storm, producing a mean accumulated precipitation of $\overline{P_a}$ = 28.23 $\pm$ 4.671 cm for the domain, meaning that 25.7% of accumulated precipitation can be attributed to graupel. That percentage is a stark contrast to the percentages for all other MPs, which range from 0.383% graupel in M2M to 8.76% graupel in WDM6. Also, MILL's standard deviation for our domain decreases by $\Delta\sigma$ = 1.703 cm when we consider graupel; this finding is largely due to sigificantly increased total accumulated precipitation east of the Connecticut River in New Hampshire, as shown in Fig. 10, which shows total accumumulated precipitation due to snow and graupel. In Fig. 10, there is minimal change from Fig. 3 in all MPs except in MILL, which now looks similar to other MPs except east of the Connecticut River, where MILL predicted more total accumulated precipitation than all other microphysics schemes.

IV Discussion

In this study, we conducted a sensitivity test of WRF MPs on a January 2019 Vermont snowstorm. We found that M2M predicted the most snowfall for our domain, Middlebury, VT, and Rochester, VT, while MILL forecasted the least snowfall out of our simulations. When compared to actual observa-

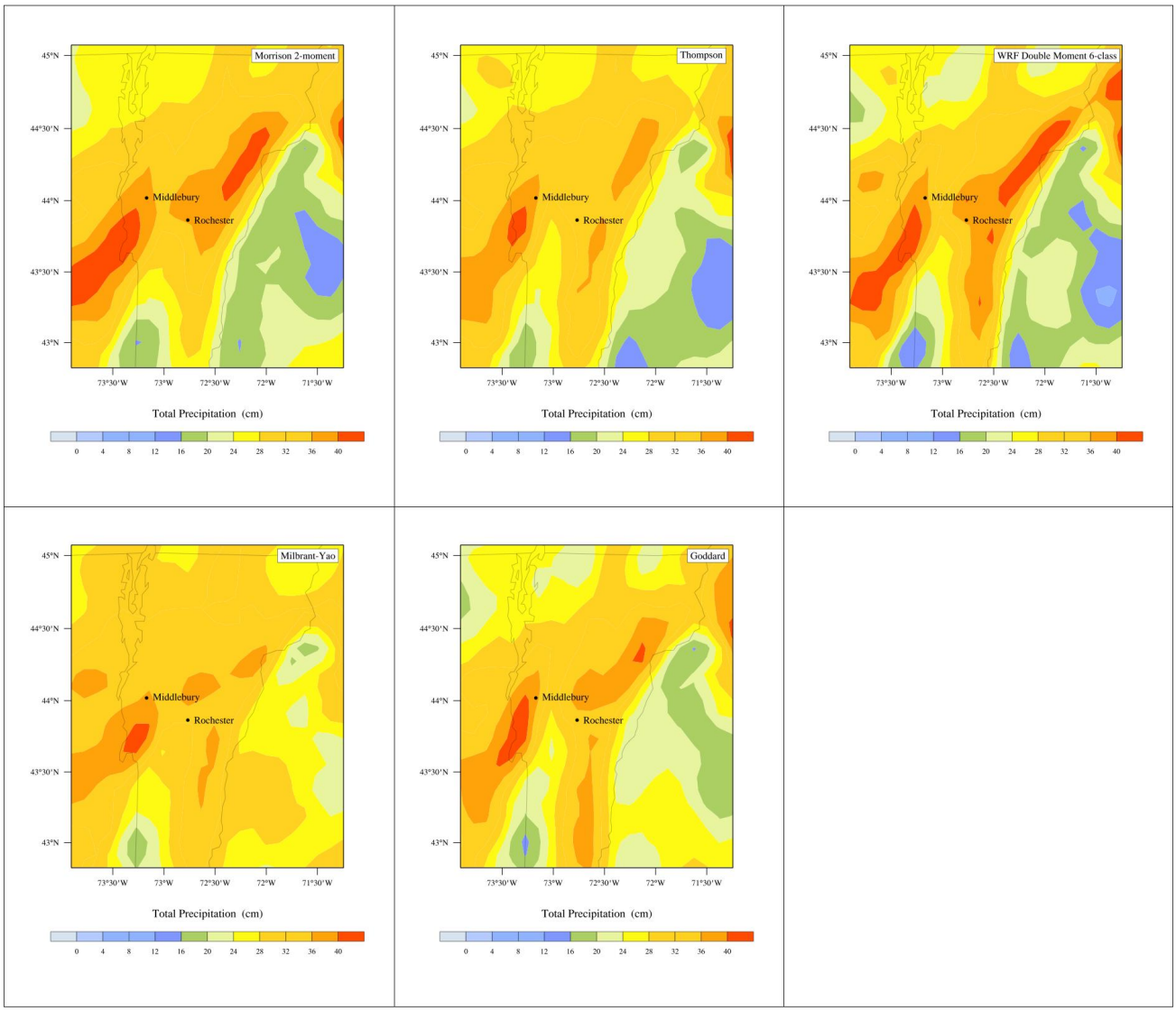

Fig. 10. As in Fig. 3, but we now include accumulation due to graupel.

tions from the storm, M2M best predicted accumulated snowfall in Middlebury, and THOM, WDM6, and GODD all predicted S_a within 0.46 cm of the observed snowfall in Rochester.

Initially, it appeared that MILL grossly underpredicted snowfall compared to all other MPs in this study. However, when we considered graupel in addition to snow, MILL predicted a total accumulated precipitation that is similar to all other MPs and actual storm observations. Actual storm data are recorded as "Total Accumulated Snowfall" or "Total Precipitation", so it is difficult to quantify the predictive power of MILL in this simulation. In other words, there are no storm data which recorded accumulated precipitation by hydrometeor. As a result, we are left to speculate about MILL's predictive power and if it was correct to forecast that roughly 25% of accumulated precipitation was due to graupel. Likely, that is not the case, and less than 10% of P_a in this storm was graupel, since all other MPs predicted that less than 10% of P_a was due to graupel and temperatures were very cold

near Earth's surface. (Graupel tends to form when there is warm air near the surface of Earth and cold air aloft). Ultimately, MILL's presumable overprediction of graupel and underprediction of snow is inconsequential in terms of making weather forecasts, because both accumulate similarly, and have the similar effects on peoples' lives.

IV. (i) The Physics of the Milbrandt-Yao Microphysics Scheme

Of the five MPs that we analyzed, the Milbrandt-Yao scheme yielded the most unique results, predicting roughly 25% of the accumulated precipitation to fall as graupel. These anomalous results motivate a further analysis of the physics behind MILL. As shown in Table I, MILL is the only three-moment microphysics scheme that we examined in this study. In addition to prognosticating hydrometeor mixing ratios q and total number concentration N_T, the MILL MP formulates a predictive equation for radar reflectivity Z, given by

$$Z = \frac{G(\alpha)}{c^2} \frac{(\rho q)^2}{N_T}, \tag{5}$$

where ρ is the density of air, c is a hydrometeor-dependent constant, and α is the shape parameter in the particle size distribution given in Eq. 2. MILL is unique from other MPs because rather than keeping α fixed, it becomes a prognosed parameter in this scheme. The shape parameter α is input in Eq. 5 through the equation

$$G(\alpha) = \frac{(6+\alpha)(5+\alpha)(4+\alpha)}{(3+\alpha)(2+\alpha)(1+\alpha)}. \tag{6}$$

With Eqs. 3- 5, there are three equations with three unknowns, which can be solved to determine α, λ, and N_0, which are input in the particle size distribution given in Eq. 2.

The principle difference between MILL and other MPs used in this study is the variation in the shape parameter α in the gamma particle size distribution $N(D)$=$N_0 D^{\alpha} e^{-\lambda D}$. If we assume that the parameters N_0 and λ remain roughly constant for each hydrometeor in different MPs, we can make an assumption about α_g and α_s for MILL. While single-moment and two-moment MPs will chose a fixed value for α_g and α_s, MILL varies these parameters. Presumably, α_g as a whole becomes greater in MILL than other MPs, which would cause a flattened, wider particle size distribution, meaning that there are more large graupel particles that can fall. And for snow, α_s on aggregate is likely less in MILL than other MPs, which causes the snow particle size distribution to have fewer particles with a large diameter D. The increased dispersion of the graupel particle size distribution caused by variation in the parameter α likely contributed to MILL's high prediction of graupel compared to all other MPs.

V Conclusion

Weather forecasting has progressed significantly since the initial development of NWP. As we continue to improve computational power and our knowledge of the atmosphere widens, bin microphysics

schemes could become operational. At the moment, though, bulk MPs underpin cloud microphysics in operational weather models, relying on a distribution to prognosticate total particle number concentrations N_T, mixing ratios q, and occasionally radar reflectivity Z for different hydrometeors. Each MP has its own tendencies and equations that predict particle sizes and fall velocities for each hydrometeor.

We conducted simulations of a January 2019 Vermont winter storm that delivered up to 50 cm of snow in parts of the state. Varying microphysics parameterizations in the Weather Research and Forecasting Model, we analyzed snowfall outputs for the storm. We found that the THOM and GODD simulations best predicted snowfall for this storm, while MILL was the big outlier, predicting much less snow than the other simulations, and underpredicting snowfall when compared to real observations at Middlebury, VT and Rochester, VT. However, considering graupel led all simulations to have fairly accurate predictions of total accumulated precipitation.

While we can conclude that the THOM and GODD simulations predicted snowfall totals that were closest to observed values at Middlebury and Rochester and that MILL was quite accurate when graupel was included, two towns is a very limited sample size for data verification, and our ability to make concrete conclusions about the "best" MP for this storm is significantly limited by our consideration of only two locations. By using more storm observations to compare each simulation to, we could make a more convincing argument about which MP choice is best for forecasting this storm and other Vermont storms. Additionally, our research used a National Center for Atmospheric Research (NCAR) Command Language (NCL) function to determine apparent radar reflectivities as determined by WRF. While we chose not to include these data in this report because they are highly dependent on the hydrometeor mixing ratios that we have already analyzed, comparing simulated radar reflectivities to actual radar data from the weather radar at Burlington International Airport (BTV) would be another way to determine which MP has the highest predictive power for this storm. It would be difficult to make a determination about which MP is "best" for winter storms in VT by only conducting a sensitivity analysis on one winter storm, as we have done. Future research could analyze multiple VT winter storms with different atmospheric conditions to see if similar trends arise.

VI Acknowledgements

I would like to thank the Middlebury College Physics department for developing me to become a scientist who asks questions about the fascinating nature of our natural world. Thanks to Professor Noah Graham for always being able to help solve the myriad of computing difficulties I had while undertaking this project and for posing exciting and perplexing new directions to take this research.

References

[1] P. Banacos and B. Taber, "The January 20-21, 2019 Winter Storm." Publisher: NOAA's National Weather Service.

[2] W. W. Grabowski, H. Morrison, S.-I. Shima, G. C. Abade, P. Dziekan, and H. Pawlowska, "Modeling of Cloud Microphysics: Can We Do Better?," *Bulletin of the American Meteorological Society*, vol. 100, pp. 655–672, Apr. 2019. Publisher: American Meteorological Society.

[3] H. Lee and J.-J. Baik, "A Comparative Study of Bin and Bulk Cloud Microphysics Schemes in Simulating a Heavy Precipitation Case," *Atmosphere*, vol. 9, p. 475, Dec. 2018. Number: 12 Publisher: Multidisciplinary Digital Publishing Institute.

[4] J. D. McMillen and W. J. Steenburgh, "Impact of Microphysics Parameterizations on Simulations of the 27 October 2010 Great Salt Lake–Effect Snowstorm," *Weather and Forecasting*, vol. 30, pp. 136–152, Feb. 2015. Publisher: American Meteorological Society.

[5] H. Morrison, G. Thompson, and V. Tatarskii, "Impact of Cloud Microphysics on the Development of Trailing Stratiform Precipitation in a Simulated Squall Line: Comparison of One- and Two-Moment Schemes," *Monthly Weather Review*, vol. 137, pp. 991–1007, Mar. 2009. Publisher: American Meteorological Society.

[6] C. Skamarock, B. Klemp, J. Dudhia, O. Gill, Z. Liu, J. Berner, W. Wang, G. Powers, G. Duda, D. Barker, and X.-y. Huang, "A Description of the Advanced Research WRF Model Version 4," 2019.

[7] J. J. Shi, W.-K. Tao, T. Matsui, R. Cifelli, A. Hou, S. Lang, A. Tokay, N.-Y. Wang, C. Peters-Lidard, G. Skofronick-Jackson, S. Rutledge, and W. Petersen, "WRF Simulations of the 20–22 January 2007 Snow Events over Eastern Canada: Comparison with In Situ and Satellite Observations," *Journal of Applied Meteorology and Climatology*, vol. 49, pp. 2246–2266, Nov. 2010. Publisher: American Meteorological Society.

[8] G. Thompson, P. R. Field, R. M. Rasmussen, and W. D. Hall, "Explicit Forecasts of Winter Precipitation Using an Improved Bulk Microphysics Scheme. Part II: Implementation of a New Snow Parameterization," *Monthly Weather Review*, vol. 136, pp. 5095–5115, Dec. 2008. Publisher: American Meteorological Society.

[9] K.-S. S. Lim and S.-Y. Hong, "Development of an Effective Double-Moment Cloud Microphysics Scheme with Prognostic Cloud Condensation Nuclei (CCN) for Weather and Climate Models," *Monthly Weather Review*, vol. 138, pp. 1587–1612, May 2010. Publisher: American Meteorological Society.

[10] J. A. Milbrandt and M. K. Yau, "A Multimoment Bulk Microphysics Parameterization. Part II: A Proposed Three-Moment Closure and Scheme Description," *Journal of the Atmospheric Sci-*

ences, vol. 62, pp. 3065–3081, Sept. 2005. Publisher: American Meteorological Society.

[11] W.-K. Tao, D. Anderson, J. Chern, J. Entin, A. Hou, P. Houser, R. Kakar, S. Lang, W. Lau, C. Peters-Lidard, X. Li, T. Matsui, M. Rienecker, M. R. Schoeberl, B.-W. Shen, J. J. Shi, and X. Zeng, "The Goddard multi-scale modeling system with unified physics," *Annales Geophysicae*, vol. 27, pp. 3055–3064, Aug. 2009.

[12] National Centers for Environmental Information (2007). "GFS Analysis, Historical 004 (0.5°)," NOAA, Dataset.